The DOI for this manuscript is doi: 10.1175/JAS-D-12-0235.1

Examination of Isentropic Circulation Response to A Doubling of Carbon Dioxide Using Statistical Transformed Eulerian Mean

Yutian Wu *

Olivier Pauluis

Courant Institute of Mathematical Sciences, New York University, New York, NY

Submitted to Journal of Atmospheric Sciences on August 20th

Revised on November 9th, 2012

* *Corresponding author address:* Yutian Wu, Courant Institute of Mathematical Sciences, New York University, New York, NY, USA

E-mail: yutian@cims.nyu.edu

ABSTRACT

Responses of the atmospheric circulation to a doubling of CO_2 are examined in a global climate model, focusing on the circulation on both dry and moist isentropes. The isentropic circulations are reconstructed using the statistical transformed Eulerian mean (STEM), which approximates the isentropic flow from the Eulerian mean and second order moments. This approach also makes it possible to decompose the changes in the circulation into changes in zonal mean and eddy statistics.

It is found that, as a consequence of CO_2 doubling, the dry isentropic circulation weakens across all latitudes. The weaker circulation in the tropics is a result of the reduction in mean meridional circulation while the reduction in eddy sensible heat flux largely contributes to the slow down of the circulation in the midlatitudes. The heat transport on dry isentropes, however, increases in the tropics because of the increase in dry effective stratification whereas it decreases in the extratropics following the reduction in eddy sensible heat transport. Distinct features are found on moist isentropes. In the tropics, the circulation weakens but without much change in heat transport. The extratropical circulation shifts poleward with an intensification (weakening) on the poleward (equatorward) flank, primarily due to the change in eddy latent heat transport. The total heat transport in the midlatitudes also shows a poleward shift but is of smaller magnitude. The differences between the dry and moist circulations reveal that in a warming world the increase in midlatitude eddy moisture transport is associated with an increase in warm moist air exported from the subtropics into the midlatitude storm tracks.

1. Introduction

As a consequence of anthropogenic climate change, the Coupled Model Inter-comparison Project phase 3 (CMIP3) models predict several robust impacts of global warming. For example, the whole troposphere is expected to extensively warm up from the deep tropics to the middle and high latitudes as well as a polar amplification at Northern Hemisphere low levels (e.g., Solomon et al. 2007). The water vapor content in the atmosphere is projected to increase significantly by about 20% for a 3 K rise of global surface temperature following the Clausius-Clapeyron relationship and assuming constant relative humidity (e.g., Held and Soden 2006). As the tropical free atmospheric temperature follows the moist adiabat, the dry static stability in the tropics increases robustly among models as the surface temperature and low-level moisture increases (e.g., Held and Soden 2006; Lu et al. 2008).

As a result of the large increase in the water vapor content in the atmosphere, the tropical circulation is expected to slow down in global warming simulations (Held and Soden 2006). They argue that for deep convection, the precipitation rate P is related to the convective mass flux M by $P = Mq$, with q the specific humidity. This amounts to assuming that air parcels leaving the boundary layer all condense and precipitate. The percentage change in convective mass flux can be written as $\frac{\delta M}{M} = \frac{\delta P}{P} - \frac{\delta q}{q} \approx \frac{\delta P}{P} - \alpha(T)\delta T$, where $\alpha \approx 0.07K^{-1}$ denoting a 7% increase in saturation vapor pressure for each 1 K temperature rise, and the approximation in the equation is due to the Clausius-Clapeyron relation and the assumption of constant relative humidity. The precipitation percentage change $\frac{\delta P}{P}$ is about $2\%K^{-1}$ and is largely constrained by the energy budget at the top of the atmosphere and at the surface. As the atmospheric water vapor increases more rapidly than the precipitation increase (i.e. $7\%K^{-1} > 2\%K^{-1}$), the overturning circulation has to slow down (i.e. $\frac{\delta M}{M} < 0$). An alternative interpretation for the weakening of the tropical mass flux stems from the balance between radiative cooling (Q) and adiabatic warming associated with descending motion in regions absent of deep convection, i.e. $Q = \omega\frac{\partial\theta}{\partial p}$, where ω is the vertical motion and θ is the potential temperature. The stratification in the troposphere ($\frac{\partial \theta}{\partial p}$) is proportional to q and thus increases at the same rate as q does. As the radiative cooling doesn't increase as rapidly as the stratification, the descending motion weakens.

The argument presented by Held and Soden (2006) pertains primarily to the Tropics. In the extratropics, the atmospheric general circulation is dominated by the eddies and is better quantified in isentropic coordinates. Indeed, the Eulerian-mean circulation in the midlatitudes is characterized by the presence of the Ferrel cell which is associated with an equatorward energy transport. In contrast, the circulation averaged on isentropic surfaces incorporates a contribution from the midlatitude eddies, akin to the Stokes' drift in gravity wave, and exhibits a single Equator-to-Pole overturning cell within each hemisphere. Characterizing the midlatitude circulation is further complicated by the fact that the isentropic circulation depends strongly on the choice made in the definition of the isentropic surfaces. Pauluis et al. (2008, 2010) show that the circulation averaged on moist isentropes - defined as surfaces of constant equivalent potential temperature - is twice as strong as the circulation on dry isentropes - defined as surfaces of constant potential temperature. The difference between the dry and moist isentropic circulation is closely tied to the transport of water vapor by the midlatitude eddies (Pauluis et al. 2010, 2011; Laliberté et al. 2012). In this paper, the changes in both the dry and moist isentropic circulations are used to characterize how the midlatitude storm tracks adjust to a warmer climate.

Laliberté and Pauluis (2010) analyzes the response of the isentropic circulations in an ensemble of CMIP3/IPCC AR4 coupled climate models under the A1B scenario. They calculated the exact isentropic circulations by summing up the meridional mass flux of air parcels with entropy less than certain values. The circulations were analyzed and compared in both dry and moist isentropes with the difference depicting the baroclinic eddies extracting warm moist air from the subtropical lower levels into the midlatitude upper troposphere (Pauluis et al. 2008). They demonstrated that, in response to global warming, the midlatitude circulation (averaged over the regions 25^oN(S)-60^oN(S)) on dry isentropes, in terms of both total mass and heat transports, consistently weakens in winter hemispheres across different models while the moist branch, defined as the difference between the dry and moist circulations, strengthens. This suggests that, in a warmer climate, the midlatitude eddies are expected to play a significant role in the atmospheric circulation by extracting a larger amount of warm and moist air from the subtropics into the midlatitudes.

In this paper, we extend the work of Laliberté and Pauluis (2010) and explore the dynamical mechanisms underlying the circulation responses on dry and moist isentropes to global warming. The dynamical mechanisms are explored by using the method of statistical transformed Eulerian-mean (STEM) recently developed in Pauluis et al. (2011). The STEM method assumes a Gaussian distribution for the joint probability density function of the meridional mass transport and provides an analytical formulation for isentropic circulations using monthly and zonal mean meridional velocity, isentropes, meridional eddy fluxes and eddy variances. The STEM isentropic circulation compares well with that of the exact calculation and can be further separated into the Eulerian-mean and the eddy components. One of the main advantages of this STEM formulation, over the conventional transformed Eulerian mean (TEM) formulation, is that it is applicable in non-stratified vertical coordinates such as the equivalent potential temperature θ_e, making the diagnosis of the circulation on moist isentropes feasible. The other improvement is that the streamlines of the STEM circulation do close above the surface. The method of STEM provides a valuable framework to analyze and understand the isentropic circulation response to global warming.

As an example of anthropogenic climate change experiment, we make use of an existing model experiment with a uniform doubling of CO_2 in the atmosphere performed on the National Center for Atmospheric Research (NCAR) Community Atmospheric Model version 3 (CAM3) coupled to a slab ocean model. It has been found in previous studies that major features of the doubling CO_2 response in the NCAR CAM3 are consistent with that in CMIP3/IPCC AR4 multi-model averages such as the broad upper tropospheric warming, the rise of the tropopause height and the poleward shift of the extratropical zonal jets and the storm tracks (Wu et al. 2012). In addition, as in Laliberté and Pauluis (2010), the changes in dry and moist isentropic circulations are quite robust among different CMIP3/IPCC AR4 climate models, especially in winter hemispheres, and the NCAR Community Climate System Model (CCSM3.0), which is a fully coupled model with higher horizontal resolution of CAM3, is one of them. This provides a certain extent of confidence in further analyzing the isentropic circulation response and its associated dynamical mechanisms within this model. Of course this technique of the STEM will eventually be applied to an ensemble of the latest generation of coupled climate models, i.e. the CMIP5, but the focus of this paper is primarily the introduction of the technique and how it works in understanding the isentropic circulation response to global warming in the NCAR CAM3. In this paper, we apply the technique of the STEM to analyze the circulation response to a doubling of CO_2 on both dry and moist isentropes. Moreover, the mechanisms underlying these changes are further examined via decomposition of the anomalies into the changes in commonly used climate variables such as the mean meridional circulation, isentropes, meridional eddy sensible and latent heat fluxes and eddy variances according the STEM formulation. Comparisons between the dry and moist isentropic circulations also provide a direct assessment of the effects of moisture in the atmospheric circulation response to global warming.

Here is the outline for this paper. In section 2, we introduce the climate model simulations that were used in this study. In section 3, the diagnostic methodology using the STEM formulation is presented. Section 4 presents the climatologies and doubling CO_2 responses in both dry and moist isentropes and in both Eulerian-mean and eddy circulations and their associated dynamical mechanisms. Discussion and conclusion is summarized in Section 5.

2. Climate Model Simulations

In this study we make use of a CO_2 doubling experiment performed using the NCAR CAM3 which is a typical IPCC AR4-class general circulation model (Collins et al. 2006).

The atmospheric model is coupled to a slab ocean model, where the ocean heat transport ('Q flux') is prescribed and the sea surface temperatures only adjust to surface energy imbalance, and a thermodynamic sea ice model. The experiment generates a pair of single- and doubled-CO_2 simulations (named $1\times CO_2$ and $2\times CO_2$ thereafter), both of which have a total of 50 ensemble runs generated with slightly perturbed initial conditions. The CO_2 concentration is fixed at 355 ppmv for the $1\times CO_2$ simulation while the $2\times CO_2$ simulation instantaneously doubles the CO_2 concentration to 710 ppmv uniformly everywhere in the atmosphere starting from January 1st. Both of the $1\times CO_2$ and $2\times CO_2$ simulations are integrated for 22 years until radiative equilibrium is reached. More information on the model itself and experimental design can be found in Wu et al. (2012).

Wu et al. (2012) and Wu et al. (2013) focused on the transient adjustment in the atmospheric zonal mean circulation immediately after the CO_2 concentration is doubled, which better reveals the dynamical mechanisms causing the circulation changes to global warming than the equilibrium response. It is found that both the tropospheric warming pattern and circulation change is well established only after a few months of integration. The tropospheric jet shift in the Northern Hemisphere (NH) takes place after a westerly anomaly in the lower stratosphere, and the authors demonstrated that this 'downward migration' process occurs via changes in linear refractive index and resulting changes in tropospheric eddy propagation in the meridional direction. In the meanwhile, the increased eddy momentum flux convergence induces an anomalous mean meridional circulation in the NH extratropics, which warms up the subtropical upper troposphere adiabatically. In the equilibrium state, a lot of global warming features found in CMIP3/IPCC AR4 models are also well simulated in the CAM3, for example, the broad tropical and subtropical upper tropospheric warming and the poleward shift of the tropospheric zonal jets and transient eddies. This provides credentials in using this model to identify the dynamical mechanisms to global warming.

The work in Wu et al. (2012) and Wu et al. (2013) is primarily based on the framework of conventional zonal mean circulation and the dry dynamics. In this paper, we aim to examine the circulation response as a consequence of CO_2 doubling in both dry and moist isentropic coordinates in the STEM framework. The dynamical mechanisms underlying these changes are also explored via decomposition of the anomalies into changes in different climate variables such as the mean meridional circulation, isentropes, eddy flux and eddy variance. The role of water vapor in the atmospheric general circulation to global warming is also investigated via comparisons between the dry and moist isentropic circulations.

In this paper, we primarily focus on boreal winter November-December-January-February (NDJF) since a large extent of consistency in isentropic circulation response exists among different CMIP3/IPCC AR4 coupled models in boreal winter (Laliberté and Pauluis 2010). The responses in boreal summer June-July-August-September (JJAS) are also analyzed and are in general agreement with the results in boreal winter. In addition, the doubling CO_2 response is defined as the difference between the $2\times CO_2$ and $1\times CO_2$ simulations while the climatologies are the results from the $1\times CO_2$ simulations. Both the climatologies and the doubling CO_2 response are averaged among the 50 ensemble runs.

3. Diagnostic Methodologies

Assuming a Gaussian distribution for the meridional mass transport's joint probability density function, Pauluis et al. (2011) derived a new method for approximating the mean meridional circulation in an arbitrary vertical coordinate and it is named the statistical transformed Eulerian-mean (STEM) formulation. In the STEM framework, isentropic streamfunction can be decomposed into the Eulerian-mean and the eddy component, i.e. $\Psi_{\xi,\mathrm{STEM}} = \Psi_{\xi,\mathrm{EUL}} + \Psi_{\xi,\mathrm{EDDY}}$, and

$$\Psi_{\xi,\mathrm{EUL}}(\overline{v},\overline{\xi},\overline{\xi'^2}) = \int_{-\infty}^{\xi} d\tilde{\xi} \int_0^{\infty} d\tilde{p} \frac{2\pi a cos\phi}{g} \frac{\overline{v}}{\sqrt{2\pi \overline{\xi'^2}}^{1/2}} \exp\Big(\frac{-(\tilde{\xi}-\overline{\xi})^2}{2\overline{\xi'^2}}\Big) \tag{1}$$

$$\Psi_{\xi,\mathrm{EDDY}}(\overline{v'\xi'},\overline{\xi},\overline{\xi'^2}) = \int_{-\infty}^{\xi} d\tilde{\xi} \int_0^{\infty} d\tilde{p} \frac{2\pi a cos\phi}{g} \frac{\overline{v'\xi'}(\tilde{\xi}-\overline{\xi})}{\sqrt{2\pi \overline{\xi'^2}}^{3/2}} \exp\Big(\frac{-(\tilde{\xi}-\overline{\xi})^2}{2\overline{\xi'^2}}\Big) \tag{2}$$

where bars denote zonal and monthly averages and primes present deviations from them. Therefore, the eddy component includes both stationary and transient eddies. The atmospheric circulation in this study is averaged on dry and moist isentropic surfaces, where ξ is the potential temperature θ and the equivalent potential temperature θ_e, respectively. The Eulerian-mean streamfunction is a function of the zonal and monthly mean meridional velocity $\overline{v}$, isentropic surfaces $\overline{\xi}$, and variance of isentropes $\overline{\xi'^2}$ (shown in Equation (1)). The eddy streamfunction is determined by the zonally and monthly averaged eddy flux $\overline{v'\xi'}$, isentropic surfaces $\overline{\xi}$, and variance of isentropes $\overline{\xi'^2}$ (shown in Equation (2)). The major advantage of the STEM method is that it can be applied in arbitrary vertical coordinates such as non-stratified θ_e surfaces as opposed to that in the framework of TEM. Also the streamlines of the STEM circulation do close at the surface.

A few quantitative measures of the isentropic circulations are the total mass transport $\Delta\Psi_\xi$, total heat transport F_ξ and effective stratification $\Delta\xi$. The total mass transport in ξ coordinate is defined as the difference between the maximum and minimum of the streamfunction at certain latitude:

$$\Delta\Psi_\xi = \max_\xi \Psi_\xi - \min_\xi \Psi_\xi \tag{3}$$

, the total meridional heat transport in ξ coordinate is written as:

$$F_\xi = \int_{-\infty}^{\infty} \tilde{\xi} \frac{\partial \Psi_{\tilde{\xi}}}{\partial \tilde{\xi}} d\tilde{\xi} \tag{4}$$

, and the effective stratification is defined as the ratio of the total meridional heat transport and the total mass transport:

$$\Delta\xi = \frac{|F_\xi|}{\Delta\Psi_\xi}. \tag{5}$$

The meridional ξ transport is conserved in ξ coordinate in the STEM formulation and is the same as that in pressure coordinate (Pauluis et al. 2011). The effective stratification can be qualitatively regarded as the thickness of the overturning cell in ξ coordinate.

In a changing climate, climate variables such as the zonal and time mean meridional velocity, isentropic surfaces, eddy fluxes and eddy variance are expected to change, all of which alter the circulation in isentropic coordinate. According to the formulation of the STEM, we decompose the anomalies in isentropic streamfunction into the contributions due to the changes in the mean meridional velocity $\overline{v}$, the eddy flux $\overline{v'\xi'}$, and the mean isentropic surface $\overline{\xi}$ and its variance $\overline{\xi'^2}$. For example, the decomposition for the Eulerian-mean streamfunction anomaly writes as:

$$
\begin{aligned}
D\Psi_{\xi,\mathrm{EUL}} &= \Psi_{\xi,\mathrm{EUL}}(\overline{v_2}, \overline{\xi_2}, \overline{\xi_2'^2}) - \Psi_{\xi,\mathrm{EUL}}(\overline{v_1}, \overline{\xi_1}, \overline{\xi_1'^2}) \\
&\approx D\Psi_{\xi,\mathrm{EUL}}(\Delta\overline{v}) + D\Psi_{\xi,\mathrm{EUL}}(\Delta\overline{\xi}) + D\Psi_{\xi,\mathrm{EUL}}(\Delta\overline{\xi'^2}),
\end{aligned}
\tag{6}
$$

with

$$D\Psi_{\xi,\mathrm{EUL}}(\Delta\overline{v}) = \Psi_{\xi,\mathrm{EUL}}(\overline{v_2}, \overline{\xi_1}, \overline{\xi_1'^2}) - \Psi_{\xi,\mathrm{EUL}}(\overline{v_1}, \overline{\xi_1}, \overline{\xi_1'^2}) \tag{7a}$$

$$D\Psi_{\xi,\mathrm{EUL}}(\Delta\overline{\xi}) = \Psi_{\xi,\mathrm{EUL}}(\overline{v_1}, \overline{\xi_2}, \overline{\xi_1'^2}) - \Psi_{\xi,\mathrm{EUL}}(\overline{v_1}, \overline{\xi_1}, \overline{\xi_1'^2}) \tag{7b}$$

$$D\Psi_{\xi,\mathrm{EUL}}(\Delta\overline{\xi'^2}) = \Psi_{\xi,\mathrm{EUL}}(\overline{v_1}, \overline{\xi_1}, \overline{\xi_2'^2}) - \Psi_{\xi,\mathrm{EUL}}(\overline{v_1}, \overline{\xi_1}, \overline{\xi_1'^2}). \tag{7c}$$

Here, $v_{1(2)}$ and $\xi_{1(2)}$ denote the climatological (perturbed) variables. In Equation (6), the change in $\Psi_{\xi,\mathrm{EUL}}$ is decomposed into the streamfunction change due to the change in the mean meridional velocity alone $D\Psi_{\xi,\mathrm{EUL}}(\Delta\overline{v})$, due to the change in the mean isentropic surface alone $D\Psi_{\xi,\mathrm{EUL}}(\Delta\overline{\xi})$, and due to the change in the variance of isentropes alone $D\Psi_{\xi,\mathrm{EUL}}(\Delta\overline{\xi'^2})$. Similarly for the anomaly in $\Psi_{\xi,\mathrm{EDDY}}$:

$$
\begin{aligned}
D\Psi_{\xi,\mathrm{EDDY}} &= \Psi_{\xi,\mathrm{EDDY}}(\overline{v_2'\xi_2'}, \overline{\xi_2}, \overline{\xi_2'^2}) - \Psi_{\xi,\mathrm{EDDY}}(\overline{v_1'\xi_1'}, \overline{\xi_1}, \overline{\xi_1'^2}) \\
&\approx D\Psi_{\xi,\mathrm{EDDY}}(\Delta\overline{v'\xi'}) + D\Psi_{\xi,\mathrm{EDDY}}(\Delta\overline{\xi}) + D\Psi_{\xi,\mathrm{EDDY}}(\Delta\overline{\xi'^2}),
\end{aligned}
\tag{8}
$$

with

$$D\Psi_{\xi,\mathrm{EDDY}}(\Delta\overline{v'\xi'}) = \Psi_{\xi,\mathrm{EDDY}}(\overline{v_2'\xi_2'}, \overline{\xi_1}, \overline{\xi_1'^2}) - \Psi_{\xi,\mathrm{EDDY}}(\overline{v_1'\xi_1'}, \overline{\xi_1}, \overline{\xi_1'^2}) \tag{9a}$$

$$D\Psi_{\xi,\mathrm{EDDY}}(\Delta\overline{\xi}) = \Psi_{\xi,\mathrm{EDDY}}(\overline{v_1'\xi_1}, \overline{\xi_2}, \overline{\xi_1'^2}) - \Psi_{\xi,\mathrm{EDDY}}(\overline{v_1'\xi_1}, \overline{\xi_1}, \overline{\xi_1'^2}) \tag{9b}$$

$$D\Psi_{\xi,\mathrm{EDDY}}(\Delta\overline{\xi'^2}) = \Psi_{\xi,\mathrm{EDDY}}(\overline{v_1'\xi_1}, \overline{\xi_1}, \overline{\xi_2'^2}) - \Psi_{\xi,\mathrm{EDDY}}(\overline{v_1'\xi_1}, \overline{\xi_1}, \overline{\xi_1'^2}) \tag{9c}$$

where the change in $\Psi_{\xi,\mathrm{EDDY}}$ is decomposed into the circulation change due to the change in the eddy flux only $D\Psi_{\xi,\mathrm{EDDY}}(\Delta\overline{v'\xi'})$, due to the change in mean isentropic surfaces only $D\Psi_{\xi,\mathrm{EDDY}}(\Delta\overline{\xi})$, and due to the change in the variance of isentropes only $D\Psi_{\xi,\mathrm{EDDY}}(\Delta\overline{\xi'^2})$. It turns out that this decomposition works well with the added contribution approximately equal the direct calculation of the anomaly (to be discussed in Results).

4. Results

In this paper, we focus primarily on boreal winter November-December-January-February (NDJF) for both hemispheres. The results are generally robust in boreal summer and will be discussed briefly at the end of this section.

a. ***Exact and STEM Isentropic Circulations***

Figure 1(a)(b) shows the climatological total STEM isentropic streamfunctions on θ and θ_e coordinates, respectively, averaged over NDJF from the CAM3-SOM $1\times CO_2$ simulations, which is the sum of the Eulerian-mean and the eddy components, i.e. $\Psi_{\theta(\theta_e),\mathrm{STEM}} = \Psi_{\theta(\theta_e),\mathrm{EUL}} + \Psi_{\theta(\theta_e),\mathrm{EDDY}}$. As a comparison, Figure 1(c)(d) shows the exact calculations of the isentropic streamfunctions by summing up the meridional mass flux with θ and θ_e less than certain values. Both the dry and moist isentropic circulations from the model simulations show a single overturning cell in each hemisphere and agree well with that of the exact calculations and the results from reanalysis datasets (see Figure 1 in Pauluis et al. 2011). In the Northern Hemisphere, while the dry isentropic circulation is dominated by a strong Hadley Cell in the tropics and a strong eddy circulation in the midlatitudes, the moist isentropic circulation strongly connects the two, spanning extensively from the deep tropics to the polar region, and maximizes in the subtropics-midlatitudes. The intensity of the moist isentropic circulation is also much larger than that of the dry one and the additional mass transport on moist isentropes corresponds to a poleward flow of warm moist air rising from the surface to the upper troposphere in the midlatitudes as demonstrated in Pauluis et al. (2008).

Figure 1(e)(f) shows the changes in the dry and moist STEM isentropic circulations as a consequence of CO_2 doubling from the model simulations, respectively. As a reference, the responses from the exact calculations are shown in Fig. 1(g)(h), where large similarities can be seen between the STEM formulation and the exact calculations except for minor differences in the upper branch of the dry circulation in the NH midlatitudes. The streamfunction $\Psi_{\theta,\mathrm{STEM}}$ shows an overall shift toward higher potential temperature. Furthermore, in the tropical regions, the potential temperature in the upper tropospheric branch increases more than the potential temperature of the surface flow. This is consistent both with a global increase in temperature and with an increase in the tropical stratification that is expected from the overall increase in water vapor content in the deep convective regions (Held and Soden 2006). We also observe an overall weakening of the dry isentropic circulation on low θ surfaces consistently across latitudes. The weakening of the circulation in the tropics is in agreement with (Held and Soden 2006) where they argued that the tropical convective mass flux is expected to slow down because of the larger increase in water vapor content than that of the precipitation. However, this argument only applies in the tropics in their study, and a key result in this paper is that the framework of isentropic circulation indicates that the weakening of the circulation extends into the midlatitudes in both hemispheres. Therefore, as a result of global warming, the general circulation of the atmosphere averaged on dry isentropes is projected to weaken across the globe, not only in the tropics, but also in the midlatitudes in both hemispheres.

The changes in $\Psi_{\theta_e,\mathrm{STEM}}$ also corresponds to a shift of the circulation toward higher value of θ_e, indicative of a significant warming and moistening of the atmosphere. In contrast to the change in the dry circulation, this upward shift is of comparable magnitude in the equatorward as in the poleward flow: the increase in low level humidity closely matches the increase in upper tropospheric potential temperature. As a result, the moist stratification does not vary noticeably. Whether it is an overall weakening or intensification of the moist circulation is hard to identify from Figure 1(f) alone. This will be further quantified later via the calculation of total mass transport. In the following, we discuss the separation of the isentropic circulation into the Eulerian-mean and the eddy components and the decomposition of their global warming anomalies into the changes in different climate variables according to the STEM formulation.

*b. **Decomposition of the STEM Isentropic Circulation Anomalies to A Doubling of Carbon Dioxide***

Using the STEM methodology as well as Equations (6) and (7), we can attribute the changes in the Eulerian-mean circulation to changes in zonal and time mean meridional velocity, isentrope and its variance. Similarly, changes in eddy circulation can be attributed to changes in zonal and time mean meridional eddy flux, isentrope and its variance, as in Equations (8) and (9). To better understand the physical mechanisms underlying the isentropic circulation response to global warming, the circulation anomalies are further decomposed into changes in different climate variables according to the STEM formulation and Equations (6)-(9).

1) **Circulation on Dry Isentropes**

Figure 2(a)(b) show the climatological Eulerian-mean ($\Psi_{\theta,\mathrm{EUL}}$) and eddy streamfunctions ($\Psi_{\theta,\mathrm{EDDY}}$) on dry isentropes during boreal winter. The Eulerian-mean circulation is comprised of a strong Hadley Cell in the tropics, spanning approximately from 30^{o}S to 30^{o}N, and a relatively weak Ferrel Cell in the extratropics in both hemispheres. The corresponding circulation anomalies in response to CO_2 doubling are shown in Figure 2(c)(d) and are largely statistically significant at above the 95% significance level among different ensemble runs (see grey shadings). To the first order, the responses in both Eulerian-mean and eddy components are characterized by an 'upward' shift towards warmer potential temperature and an overall weakening of the circulation.

We consider first the contributions to the changes in the Eulerian-mean streamfunction (shown in Fig. 2(c)). Both the changes in mean temperature and mean meridional velocity contribute to the change in the streamfunction ($D\Psi_{\theta,\mathrm{EUL}}(\Delta\overline{\theta})$ as shown in Fig. 2(e) and $D\Psi_{\theta,\mathrm{EUL}}(\Delta\overline{v})$ as shown in Fig. 2(g)), with negligible contribution from the change in the variance of θ ($D\Psi_{\theta,\mathrm{EUL}}(\Delta\overline{\theta'^2})$; not shown). The sum of these contributions is nearly equal to the difference in the circulation, suggesting that the changes in nonlinear terms remain small enough for the linear decomposition to be valid. The circulation anomaly due to the change in θ alone corresponds to the 'upward' shift of the circulation toward warmer temperature. It also reveals the increase in tropical dry stratification due to the fact that the potential temperature in the poleward flow of the Hadley Cell increase more than the equatorward flow at the surface (shown in Fig. 2(e)). The streamfunction anomaly due to the change in mean meridional velocity (shown in Fig. 2(g)), corresponds to a weakening of the Hadley Cell and a poleward shift of the NH Ferrel Cell with a strengthening (weakening) of the circulation on the poleward (equatorward) flank of the jet. The poleward shift of the NH Ferrel Cell is consistent with the poleward shift of the midlatitude storm tracks to increased greenhouse warming found in previous studies (e.g., Yin 2005).

Similarly applying the STEM methodology (Equations (8) and (9)) to the CO_2 doubling response in $\Psi_{\theta,\mathrm{EDDY}}$, the change in $\Psi_{\theta,\mathrm{EDDY}}$ is largely attributed to the change in temperature as well as eddy sensible heat flux ($D\Psi_{\theta,\mathrm{EDDY}}(\Delta\overline{\theta})$ as shown in Fig. 2(f) and $D\Psi_{\theta,\mathrm{EDDY}}(\Delta\overline{v'\theta'})$ as shown in Fig. 2(h)). The streamfunction change due to the change in $\overline{\theta}$ alone again shows an 'upward' shift of the eddy circulation towards higher θ surfaces for both hemispheres (shown in Fig. 2(f)). As noted above, this shift is more pronounced in the upper troposphere than near the surface, resulting in a deepening of the circulation in dry isentropic coordinates. As shown in Fig. 2(h), a weakening of the eddy sensible heat flux occurs in both hemispheres and contributes to a broad weakening of the isentropic circulation in the midlatitudes. This decrease in midlatitude eddy sensible heat flux is a result of reduction in both stationary and transient eddies (to be shown later in Figure 6(a)). The contribution due to the change in the variance alone is again small compared to other terms (not shown).

2) **Circulation on Moist Isentropes**

Figure 3 shows the changes on the circulation averaged on moist isentropes θ_e. Because of the smaller vertical variation in θ_e in the tropics and some cancellation of the lower and upper tropospheric flow with the same value of θ_e, the climatological tropical Hadley Cell on moist isentropes is shallower and spans over a smaller range of θ_e than that on dry isentropes (shown in Fig. 3(a)). The climatological eddy circulation on moist isentropes includes both sensible and latent heat transports associated with the eddies and thus is much stronger than that on dry isentropes (shown in Fig. 3(b)). The difference between the dry and moist isentropic circulations reveals the moisture transport carried out by the eddies which play an important role in extracting water vapor from the subtropics into the midlatitudes (Pauluis et al. 2008).

The response in $\Psi_{\theta_e,\mathrm{EUL}}$ to CO_2 doubling and its decomposition based on the STEM formulation are shown in Figure 3 (left). The features are broadly consistent with that on dry isentropes except for the narrower structure: the circulation generally shifts towards larger θ_e values over the entire globe, primarily due to the change in $\overline{\theta_e}$ (shown in Fig. 3(e)), and the Hadley circulation slightly weakens and the NH Ferrel Cell moves towards higher latitudes because of the change in mean meridional flow (shown in Fig. 3(g)). When comparing with the corresponding on dry isentropes (Fig. 2(c) and Fig. 3(c)), we note that the main difference lies in that the increase in equivalent potential temperature is similar in the poleward and equatorward branch (while the increase in potential temperature is larger in the poleward branch of the circulation) which suggests that changes in the atmospheric stratification are closely tied to the low level equivalent potential temperature response, even outside the tropics.

The change in the eddy contribution $\Psi_{\theta_e,\mathrm{EDDY}}$ is much larger than the corresponding changes in the dry circulation $\Psi_{\theta,\mathrm{EDDY}}$ and spans extensively from the deep tropics to the polar regions (shown in Fig. 3(d)). It is dominated by the streamfunction change due to the change in $\overline{\theta_e}$ alone, which shows an 'upward' shift towards larger values of θ_e and indicates the substantial moistening of the atmosphere in addition to warming (shown in Fig. 3(f)). In addition, as shown in Fig. 3(h), the streamfunction change due to the change in $\overline{v'\theta_e'}$ shows a weakening of the eddy circulation in the subtropics but a strengthening in the middle and high latitudes for both hemispheres. This is in strong contrast with the changes for the circulation on dry isentropes which shows an overall weakening of the eddy circulation (shown in Fig. 2(h)). This suggests that, despite a weakening of the eddy sensible heat flux, the meridional latent heat transport associated with the eddies significantly intensifies in the middle and high latitudes and compensates for the reduction in eddy sensible heat flux in these regions. This translates into an intensification of the circulation on moist isentropes in middle and high latitudes.

Pauluis et al. (2008) presented the atmospheric zonal mean circulation on moist isentropes and showed from reanalysis datasets that the long-term mean circulation on moist isentropes is about twice as large as that on dry isentropes. Here we have shown that the circulations on dry and moist isentropes respond differently to an increase in greenhouse gas concentration. The dry circulation shows an overall weakening, which is tied both to weakening of the Hadley cell in the tropics and to a reduction of the eddy transport of sensible heat in the midlatitudes. In contrast, the circulation on moist isentropes weakens in the tropics and subtropical regions, but intensifies in in the midlatitudes and polar regions. The midlatitudes changes is dominated by the increase in the poleward eddy transport of moisture.

c. *Changes in Total Mass and Heat Transport*

1) **Circulation on Dry Isentropes**

The changes in dry and moist isentropic circulations are further quantified through the measure of total mass transport $\Delta\Psi$ and total heat transport F for both the Eulerian-mean and the eddy components and the sum of the two.

Figure 4(a) shows the climatological and anomalous Eulerian-mean mass transport on dry isentropes and its decomposition into the changes in $\overline{v}$, $\overline{\theta}$, and $\overline{\theta'^2}$. It turns out that the contributions from the changes in $\overline{\theta}$ and $\overline{\theta'^2}$ are small and the total mass transport anomaly is mainly attributed to the change in the mean meridional flow. The intensity of the Hadley Cell, measured by the maximum mass transport, in general weakens, and this is in agreement with the global warming response found in CMIP3/IPCC AR4 coupled climate models (Held and Soden 2006). The NH Ferrel Cell shifts slightly poleward and intensifies on the poleward flank of its climatological position. The change in Eulerian-mean energy transport is, however, different from that in mass transport, especially in the tropics, and is shown in Fig. 4(b). Indeed, an increase in atmospheric stratification makes it possible for weaker mass flux to result in an enhanced heat transport, as can be noticed in the NH. One can also observe an increase in the divergence of heat transport on the northern side of the Equator, which is most likely associated with enhanced precipitation in these regions. Note also that the poleward shift of the NH Ferrel cell corresponds to an equatorward heat transport at high latitudes. Figure 4(c)(d) shows the changes for the eddy circulation and the attributions to the changes in $\overline{\theta}$, $\overline{\theta'^2}$ and $\overline{v'\theta'}$. The total mass and heat transport in the eddy circulation decrease in the extratropics in both hemispheres, especially the NH, which are primarily due to the reduction in eddy sensible heat flux.

The sum of the Eulerian-mean and the eddy circulations is shown in Figure 4(e)(f). The total mass transport decreases across all latitudes especially in the tropics and the NH midlatitudes. The weaker circulation within the tropics is primarily due to the weakening of the mean meridional circulation while the weakening in the midlatitudes is a result of reduction in meridional eddy sensible heat flux. The total heat transport overall intensifies within the Hadley Cell as a result of the dry stratification increase in the tropics despite weaker mass transport. The poleward heat transport decreases in the NH midlatitudes as a result of both the reduction in poleward heat transport by the eddies and the increase in equatorward heat transport by the Ferrel Cell. The percentage decrease is larger for the total heat transport in the midlatitudes than that of the total mass transport, which implies a reduction in dry effective stratification in these regions.

2) **Circulation On Moist Isentropes**

The changes in the circulation on moist isentropes, shown in Figure 5, are quite different from the changes of the circulation averaged on dry isentropes circulation. The climatological Eulerian-mean mass and heat transport is smaller on moist isentropes because the relatively high value of equivalent potential temperature near the surface results in a partial compensation between the lower and upper level flow when the circulation is varied on θ_e surfaces. It is found that, as a consequence of CO_2 doubling, the Eulerian-mean mass transport $\Delta\Psi_{\theta_e,\mathrm{EUL}}$ weakens in the tropics, primarily because of the change in mean meridional circulation. The Eulerian-mean heat transport $F_{\theta_e,\mathrm{EUL}}$, however, doesn't change much within the Hadley Cell: there is a strong degree of compensation between an increased equatorward moisture transport and an increased poleward potential temperature transport as shown in Fig. 4(b). In the NH midlatitudes, both the total mass and heat transports increase but the latter with smaller percentage increase relative to the climatology.

The climatological mass transport by the eddies on moist isentropes is approximately twice as large as that on dry isentropes in the midlatitudes (shown in Fig. 4(c) and Fig. 5(c)), in good agreement with Pauluis et al. (2008). The change in eddy mass transport shows a poleward shift in both hemispheres with a reduction of mass transport equatorward of the climatological maximum location, i.e. at about 40^o in each hemisphere, and an increase poleward of it. This change is due to both the changes in $\overline{\theta_e}$ and $\overline{v'\theta_e'}$, both of which contribute to the poleward shift of the mass transport. The mass transport change due to the change in $\overline{\theta_e'^2}$ alone is an increase in the NH midlatitudes but a decrease in the SH midlatitudes. Similarly for the change in $F_{\theta_e,\mathrm{EDDY}}$, it also shows a poleward shift, as a result of both the changes in $\overline{\theta_e}$ and $\overline{v'\theta_e'}$, but is of much smaller percentage change in comparison to that in total mass transport.

Figure 5(e)(f) shows the response in total mass and heat transport calculated from the sum of $\Psi_{\theta_e,\mathrm{EUL}}$ and $\Psi_{\theta_e,\mathrm{EDDY}}$. The change in total mass transport generally decreases in the tropics but shows a poleward shift in the midlatitudes for both hemispheres. The total heat transport generally decreases except at middle and high latitudes, but it is comparatively smaller than the change in the mass transport. This implies an increase in moist effective stratification at low latitudes while a reduction in the NH middle and high latitudes.

This analysis of the moist circulation indicates that while the midlatitudes eddies would transport less sensible heat, this is, in large part, compensated by a higher water vapor transport. This compensation is not complete, but is in fact associated with a slight poleward shift in total energy transport. Furthermore, in contrast to the dry circulation which weakens through the entire globe, the moist circulation shows a significant intensification in the middle and high latitudes. The increase in mass transport in these regions cannot be explained by the increase in poleward heat flux alone, but is due, in a significant part, to a reduction in the effective stratification for equivalent potential temperature. From a physical point of view, this is likely due to the poleward intensification which results in an enhanced warming and moistening of low level air masses at high latitudes. As these air masses are advected equatorward with higher values of θ_e, a larger total mass transport is then necessary to achieve the same amount of heat transport.

The global warming responses simulated by the NCAR CAM3-SOM are broadly consistent with the results in CMIP3/IPCC AR4 coupled models such as the weakening of the tropical circulation. However, there is some discrepancy in the change of the poleward atmospheric energy transport in this model. As found in Held and Soden (2006), the atmospheric energy transport, averaged across CMIP3/IPCC AR4 models, increases across the globe with increased poleward dry static energy dominating in the tropics and increased eddy latent heat transport dominating in the extratropics. On the contrary, the total heat transport in the CAM3-SOM in response to CO_2 doubling generally decreases except at middle and high latitudes, and this is consistent with the energy flux change at the top of the atmosphere (TOA) (not shown). This discrepancy in the CAM3-SOM simulations is probably related to the negative cloud feedback in this model and in equilibrated state less energy is required to transport out of the tropics. Zhang and Bretherton (2008) noted the negative cloud feedback in this model and the underlying mechanisms were explored by using an idealized single-column model with prescribed large-scale forcing conditions. It was found that both the higher cloud liquid water content in stratiform clouds and the longer cloud life cycle contribute to the negative cloud feedback in this model. It is noted here that we have in mind that certain biases may exist in one single model, and eventually we will extend this STEM decomposition analysis to an ensemble of CMIP5 coupled climate models to examine the robustness of the results in this paper.

3) **Moisture transport**

It has been widely recognized that the water vapor will play an important role in the future warming climate (e.g., Held and Soden 2006). In this paper, we analyze the role of moisture by comparing the isentropic circulations on dry and moist isentropes, especially the circulation accomplished by the eddies. As in Laliberté and Pauluis (2010), the moist branch in the eddy circulation is defined as the difference between the dry and moist isentropic circulations, i.e. $\Psi_{\theta_e,\mathrm{EDDY}} - \Psi_{\theta,\mathrm{EDDY}}$. Figure 6 shows the total mass and heat transport and their response to CO_2 doubling in both dry and moist branches by the eddies. To better understand the dynamics, the response in transient and stationary eddies is also shown. As mentioned above, both the mass and heat transport in the dry branch decrease, which is a result of the weakening of both stationary and transient eddies (shown in Fig. 6(a)(b)). The transient eddy sensible heat flux decreases in the lower troposphere in northern winter and this is probably because of the strong polar amplification and resulting reduction in meridional temperature gradient at low levels (not shown). The sensible heat flux by the stationary waves is also found to decrease in this model as a consequence of global warming. In comparison, the change in total mass transport within the moist branch shows a poleward shift in both hemispheres with increased (decreased) mass transport poleward (equatorward) of 30^{o}N and 40^{o}S. This is primarily due to the change in transient eddies in the subtropics and midlatitudes, and to a lesser extent, the change in stationary waves in the NH higher latitudes. The eddy latent heat transport is found to intensify in both hemispheres largely due to the response in transient eddies in the midlatitudes, and to a lesser extent, the change in stationary waves in the subtropics and NH higher latitudes. Compared to the change in the dry branch, the increased heat transport in the moist branch shows a large compensation with the reduction in the dry one. This compensation between the change in dry static energy and the change in latent heat transport in response to global warming was also found in CMIP3/IPCC AR4 multi-model averages in Held and Soden (2006).

d. ***Results for Boreal Summer June-July-August-September***

Figures 7-10 show the corresponding results for boreal summer averaged over June-July-August-September (JJAS) from the CAM3-SOM doubling CO_2 simulations. The STEM isentropic circulation agrees well with that of the exact calculation on both dry and moist isentropes during JJAS (shown in Figure 7), thus understanding the circulation response to a doubling of CO_2 using the STEM formulation is valid. The CO_2 doubling response using the STEM formulation is also similar to that of the exact calculation (not shown), which shows a similar weakening of the dry isentropic circulation across all latitudes in both hemispheres as well as an 'upward' shift towards larger values of θ, especially in the tropics (shown in Fig. 7(e)). In comparison, the change in moist isentropic circulation is of larger amplitude and shows an extensive 'upward' shift from the deep tropics to the polar regions in both hemispheres (shown in Fig. 7(f)).

The isentropic circulation is further separated into the Eulerian-mean and the eddy components, and the STEM decomposition of their streamfunction anomalies during boreal summer is shown in Figure S1 and S2. The responses on both dry and moist isentropes are largely similar to the results in boreal winter and show a general weakening of the dry circulation across all latitudes while an intensification of the moist circulation in the middle and high latitudes, especially for the SH. To better quantify the circulation, Figure 8 shows the climatological total mass and heat transports and their responses to CO_2 doubling on dry isentropes. The dry circulation in the tropics weakens, due to the reduction in mean meridional circulation (shown in Fig. 8(a)); the total heat transport, however, in general increases in the tropics because of the increase in dry effective stratification (shown in Fig. 8(b)). In the extratropics, both the total mass and heat transports decrease, mainly as a result of the reduction in eddy sensible heat flux (shown in 8(c)(d)). The change in mean isentropic surfaces also contributes to the weakening of the eddy circulation in the SH midlatitudes.

The moist isentropic circulation is found to respond differently and is shown in Figure 9. Because of the cancellation between the increased poleward dry static energy and the increased equatorward moisture transport, there is little change in the Eulerian-mean total heat transport in the tropics. In the extratropics, the changes in both mass and heat transports in the eddy circulation show a poleward shift, especially in the SH midlatitudes with intensification (reduction) poleward (equatorward) of 40^oS. The eddy circulation in general weakens in the NH extratropics except for a slight intensification poleward of 60^oN.

Figure 10 shows the eddy circulation anomaly in the moist branch, together with the results in the dry branch during boreal summer. While the total mass transport in the dry branch shows a reduction in both hemispheres, the moist branch shows a poleward shift with an intensification (reduction) poleward (equatorward) of about 40^oN(S), primarily due to the change in transient eddies. The total heat transport in the dry branch decreases in both hemispheres due to the weakening of both stationary and transient eddies. In contrast, the meridional eddy latent heat transport intensifies across the globe, as a result of the change in transient eddies in the SH and in both transient and stationary waves in the NH. This, to some extent, compensates the reduction in the dry circulation.

5. Discussion and Conclusion

The atmospheric general circulation averaged on isentropic surfaces is expected to change in a warmer climate. Laliberté and Pauluis (2010) found that, in response to rising greenhouse gases, the circulation on dry isentropes, averaged in the midlatitudes, is projected to weaken while the difference between the dry and moist isentropic circulations strengthens in wintertime. The results are quite robust for an ensemble of CMIP3/IPCC AR4 coupled climate models under the A1B scenario. In this paper, we aim to better understand the dynamical mechanisms underlying the circulation changes on dry and moist isentropes to global warming by focusing on an ensemble of equilibrium integrations from the NCAR CAM3 coupled to a slab ocean model as a result of CO_2 doubling. We apply the newly developed STEM methodology to analyze the circulation on both dry and moist isentropes with the difference depicting the effects of water vapor. The STEM formulation also separates the isentropic circulation into the Eulerian-mean circulation, which dominates in the tropics, and the eddy circulation which maximizes in the extratropics. Following the formulation of the STEM, the isentropic circulation response to CO_2 doubling is further decomposed into the circulation change due to the change in commonly used zonal and monthly mean climate variables such as the mean isentrope, meridional velocity, meridional eddy fluxes and eddy variance.

The Eulerian-mean circulation on dry isentropes is dominated by the strong Hadley circulation in the tropics, which weakens as a consequence of CO_2 doubling, largely due to the weakening of the mean meridional circulation. This is in agreement with Held and Soden (2006) where they interpreted the weakening of the tropical circulation as a result of faster increase in water vapor content than that of the precipitation. Despite the weakening of the tropical circulation, the total heat transport in general strengthens, suggesting an increase in dry effective stratification in the tropics. More importantly in this paper, we found that the weakening of the Hadley Cell extends to the midlatitudes when one considers the circulation averaged on dry isentropes. It is found that both the total mass and heat transports in the eddy circulation weaken in the extratropics, primarily as a result of the weakening in sensible heat flux by the stationary and transient eddies. The larger percentage reduction in heat transport than that in mass transport suggests a decrease in dry effective stratification in the NH middle and high latitudes.

Furthermore, the circulation responses have a distinct manifestation on moist isentropes compared to the results on dry ones. The tropical Hadley Cell also weakens on moist isentropes but without much change in total heat transport due to the large compensation between the increased equatorward moisture transport and the increased poleward dry static energy transport. In the extratropics, the eddy circulation on moist isentropes displays a poleward shift with an intensification (reduction) on the poleward (equatorward) flank for both hemispheres. This can be attributed to the changes in meridional eddy equivalent potential temperature transport and mean moist isentropic surface. The total heat transport associated with the eddies also shows a poleward shift but is of smaller magnitude than that of the mass transport, implying a decrease in moist effective stratification in the extratropics.

The different responses between the dry and moist isentropic circulations in the midlatitudes are closely related to the change in poleward moisture transport by the eddies. The moist branch, which is defined as the difference between the dry and moist eddy circulations, significantly intensifies in the middle and high latitudes while weakening in the subtropics, as a result of both stationary and transient eddies extracting more water vapor from the subtropics to the middle and high latitudes. The intensification of the moist branch indeed dominates over the weakening of the dry circulation, leading to the poleward shift of the moist isentropic circulation in the extratropics. As for heat transport, there is a large degree of compensation between the intensified poleward moisture transport and the reduced sensible heat transport, which is also consistent with the results in Held and Soden (2006).

This study points to the importance of diagnosing the atmospheric general circulation on both dry and moist isentropes. Depicting the circulation and its response on dry isentropes alone could be misleading in this context. Compared to the dry isentropic circulation, the moist circulation includes the meridional eddy latent heat flux which significantly changes in a warmer climate and affects the general circulation response to global warming. While the dry circulation in general weakens across the globe, the moist branch intensifies and, in fact, to a large extent, compensates the reduction in the dry branch. This implies that, in a warmer climate, the storm tracks would extract more warm moist air masses from the subtropics, leading to enhance precipitation in the midlatitudes.

One caveat of this study is the use of one single model and the model's possible biases. As discussed above, as opposed to the increased global atmospheric poleward energy transport found in most CMIP3/IPCC AR4 coupled climate models and atmospheric models with slab ocean models (Held and Soden 2006; Hwang and Frierson 2010), the total energy transport in the NCAR CAM3 coupled to a slab ocean model generally decreases except at the middle and high latitudes. This is probably related to the negative cloud feedback in this model (Zhang and Bretherton 2008), which tends to reduce the atmospheric heat transport out of the tropics. Therefore, an extension to an ensemble of CMIP5 coupled climate models is of necessity. The robustness of the results shown in this paper will be discussed, in particular, the contributions from the stationary and transient eddies in determining the change in total mass and heat transport, and also the change in dry and moist effective stratification and its underlying physical mechanisms.

Acknowledgments.

The authors are grateful to Prof. Ming Cai and two anonymous reviewers for their helpful comments on the manuscript. Olivier Pauluis and Yutian Wu have been supported by the NSF under Grant AGS-0944058 for this work.

REFERENCES

Collins, W. D., et al., 2006: The formulation and atmospheric simulation of the Community Atmosphere Model version 3 (CAM3). *J. Clim.*, **19**, 2144–2161.

Held, I. M. and B. J. Soden, 2006: Robust Response of the Hydrological Cycle to Global Warming. *J. Clim.*, **19**, 5686–5699.

Hwang, Y.-T. and D. M. W. Frierson, 2010: Increasing atmospheric poleward energy transport with global warming. *Geophys. Res. Lett.*, **37**, L24 807, doi:10.1029/2010GL045 440.

Laliberté, F. and O. Pauluis, 2010: Winter intensification of the moist branch of the circulation in simulations of 21st century climate. *Geophys. Res. Lett.*, **37**, L20 707, doi:10.1029/2010GL045 007.

Laliberté, F., T. A. Shaw, and O. Pauluis, 2012: Moist recirculation and water vapor transport on dry isentropes. *J. Atmos. Sci.*, **69**, 875–890.

Lu, J., G. Chen, and D. M. W. Frierson, 2008: Response of the zonal mean atmospheric circulation to El Nino versus global warming. *J. Clim.*, **21**, 5835–5851.

Pauluis, O., A. Czaja, and R. Korty, 2008: The global atmospheric circulation on moist isentropes. *Sci.*, **321**, 1075–1078, doi:10.1126/science.1159 649.

Pauluis, O., A. Czaja, and R. Korty, 2010: The global atmospheric circulation in moist isentropic coordinates. *J. Clim.*, **23**, 3077–3093.

Pauluis, O., T. A. Shaw, and F. Laliberté, 2011: A statistical generalization of the transformed Eulerian-mean circulation for an arbitrary vertical coordinate system. *J. Atmos. Sci.*, **68**, 1766–1783.

Solomon, S., D. Qin, M. Manning, Z. Chen, M. Marquis, K. B. Averyt, M. Tignor, and H. L. M. (eds.), 2007: Contribution of Working Group I to the Fourth Assessment Report of the Intergovernmental Panel on Climate Change, 2007. Cambridge University Press, Cambridge, United Kingdom and New York, NY, USA.

Wu, Y., R. Seager, T. A. Shaw, M. Ting, and N. H. Naik, 2013: Atmospheric circulation response to an instantaneous doubling of carbon dioxide Part II: Atmospheric transient adjustment and its dynamics. *J. Clim.*, doi:10.1175/JCLI–D–12–00 104.1, in press.

Wu, Y., R. Seager, M. Ting, N. H. Naik, and T. A. Shaw, 2012: Atmospheric circulation response to an instantaneous doubling of carbon dioxide Part I: Model experiments and transient thermal response in the troposphere. *J. Clim.*, **25**, 2862–2879.

Yin, J. H., 2005: A consistent poleward shift of the storm tracks in simulations of 21st century climate. *Geophys. Res. Lett.*, **32**, L18 701, doi:10.1029/2005GL023 684.

Zhang, M. and C. S. Bretherton, 2008: Mechanisms of low cloud climate feedback in idealized single-column simulations with the Community Atmospheric Model (CAM3). *J. Clim.*, **21**, 4859–4878.

List of Figures

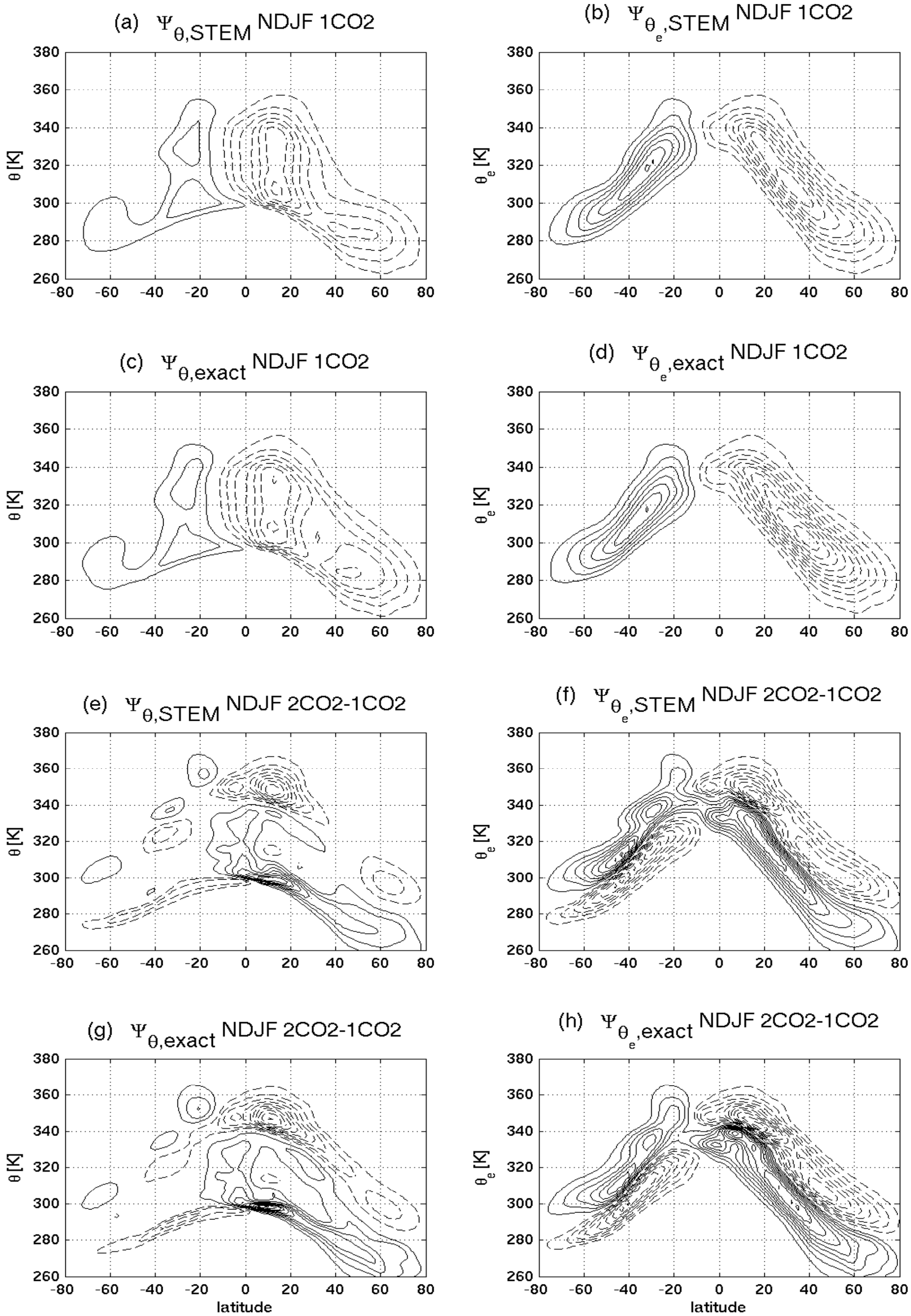

FIG. 1. The climatological streamfunctions on dry and moist isentropes calculated based on the statistical transformed Eulerian-mean (STEM) formulation during November-December-January-February (NDJF) from the CAM3-SOM $1\times CO_2$ simulations (a)(b). Same as (a)(b) but for the exact calculations of the isentropic streamfunction (c)(d). The doubling CO_2 response on dry and moist isentropes from the STEM methodology (e)(f), and from the exact calculation (g)(h). The contour intervals are 2×10^{10} kg/s for (a)-(d), and 0.5×10^{10} kg/s for (e)-(h), and negative contours representing clockwise motion are dashed.

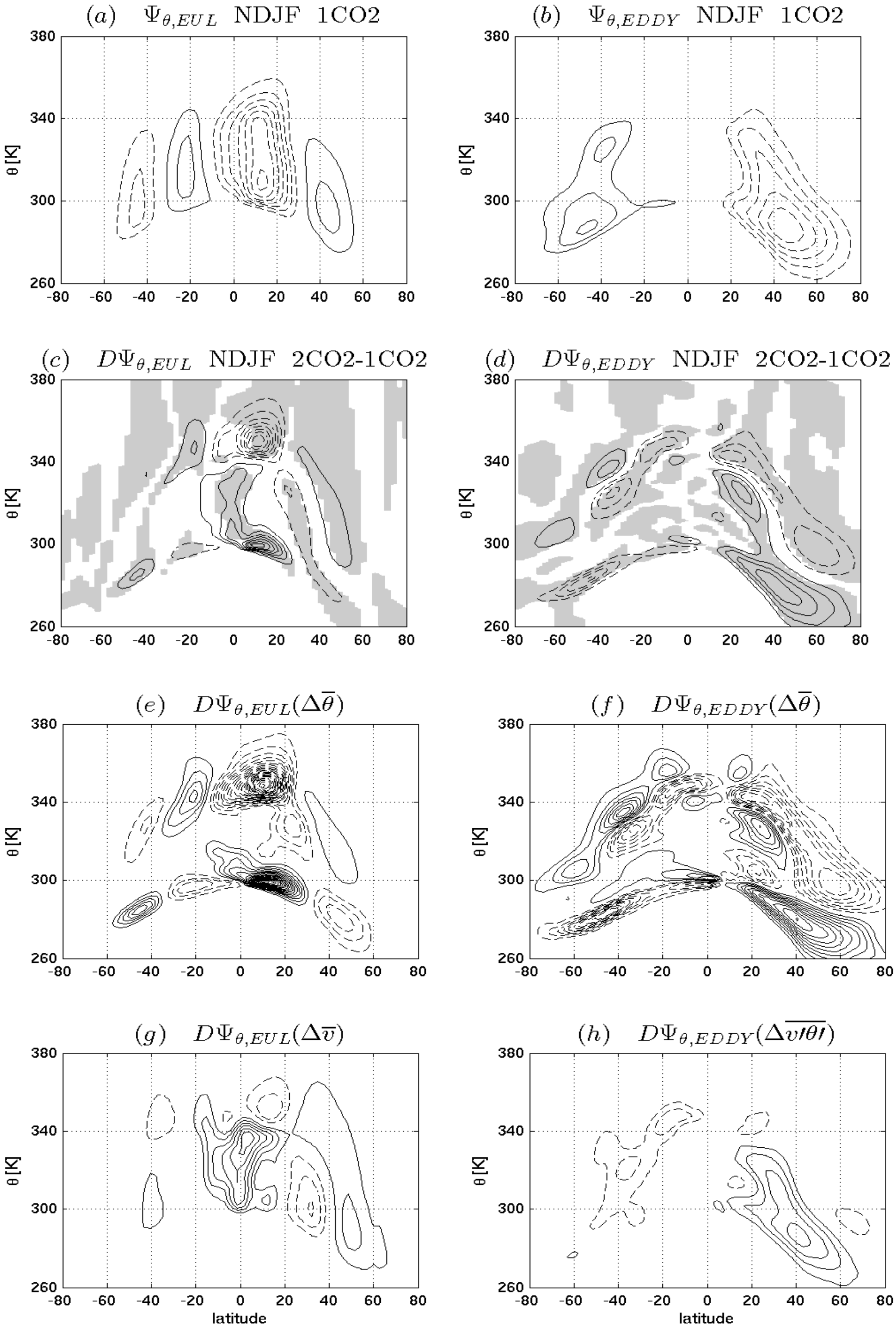

FIG. 2. Decomposition of the changes in isentropic streamfunction for $\Psi_{\theta,\mathrm{EUL}}$ (left) and $\Psi_{\theta,\mathrm{EDDY}}$ (right). (a) The climatological $\Psi_{\theta,\mathrm{EUL}}$ and (c) its doubling CO_2 response. The decomposition into the changes in (e) $\overline{\theta}$ alone and (g) $\overline{v}$ alone. The same for the eddy circulation except for (h) showing the streamfunction change due to the change in $\overline{v'\theta'}$. The contour intervals are 2×10^{10} kg/s for (a)(b), 0.5×10^{10} kg/s for (c)(d) and 0.2×10^{10} kg/s for others. The grey shadings in (c)(d) indicate the 95% statistical significance.

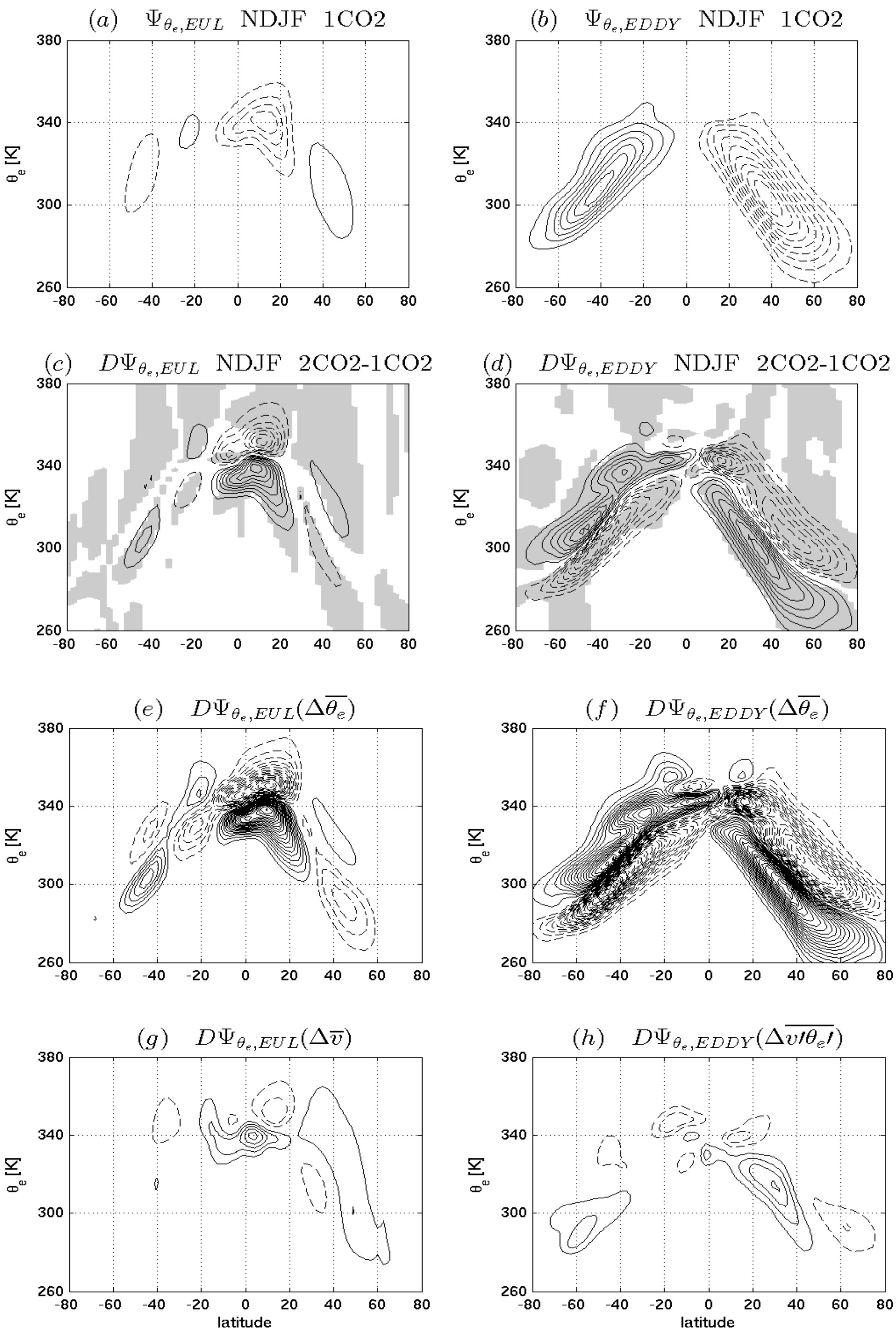

FIG. 3. Same as Figure 2 but for the circulation on moist isentropes.

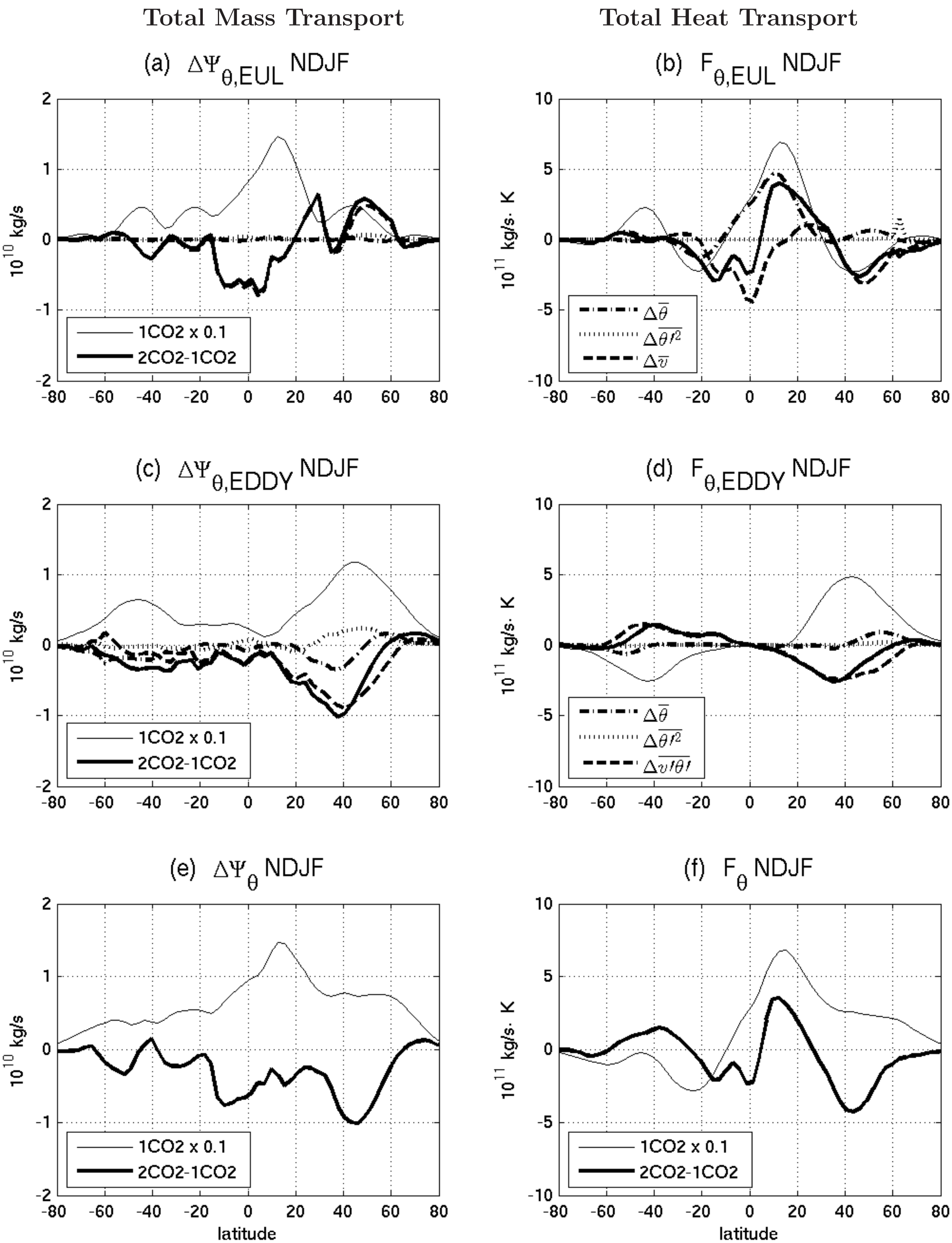

FIG. 4. The changes in Eulerian-mean mass transport $\Delta\Psi_{\theta,\mathrm{EUL}}$ (a) and heat transport $F_{\theta,\mathrm{EUL}}$ (b) on dry isentropes and their decomposition into the changes in $\overline{\theta}$ (dash-dot line), $\overline{\theta'^2}$ (dotted line) and $\overline{v}$ (dashed line), as indicated in legend, and is shown in the first row. The same for the second row but for $\Delta\Psi_{\theta,\mathrm{EDDY}}$ (c) and $F_{\theta,\mathrm{EDDY}}$ (d) and the decomposition into $\overline{\theta}$ (dash-dot line), $\overline{\theta'^2}$ (dotted line) and $\overline{v'\theta'}$ (dashed line). The sum of the Eulerian-mean and the eddy components is shown in the third row. The climatologies are also plotted in thin solid lines but are divided by a factor of 10.

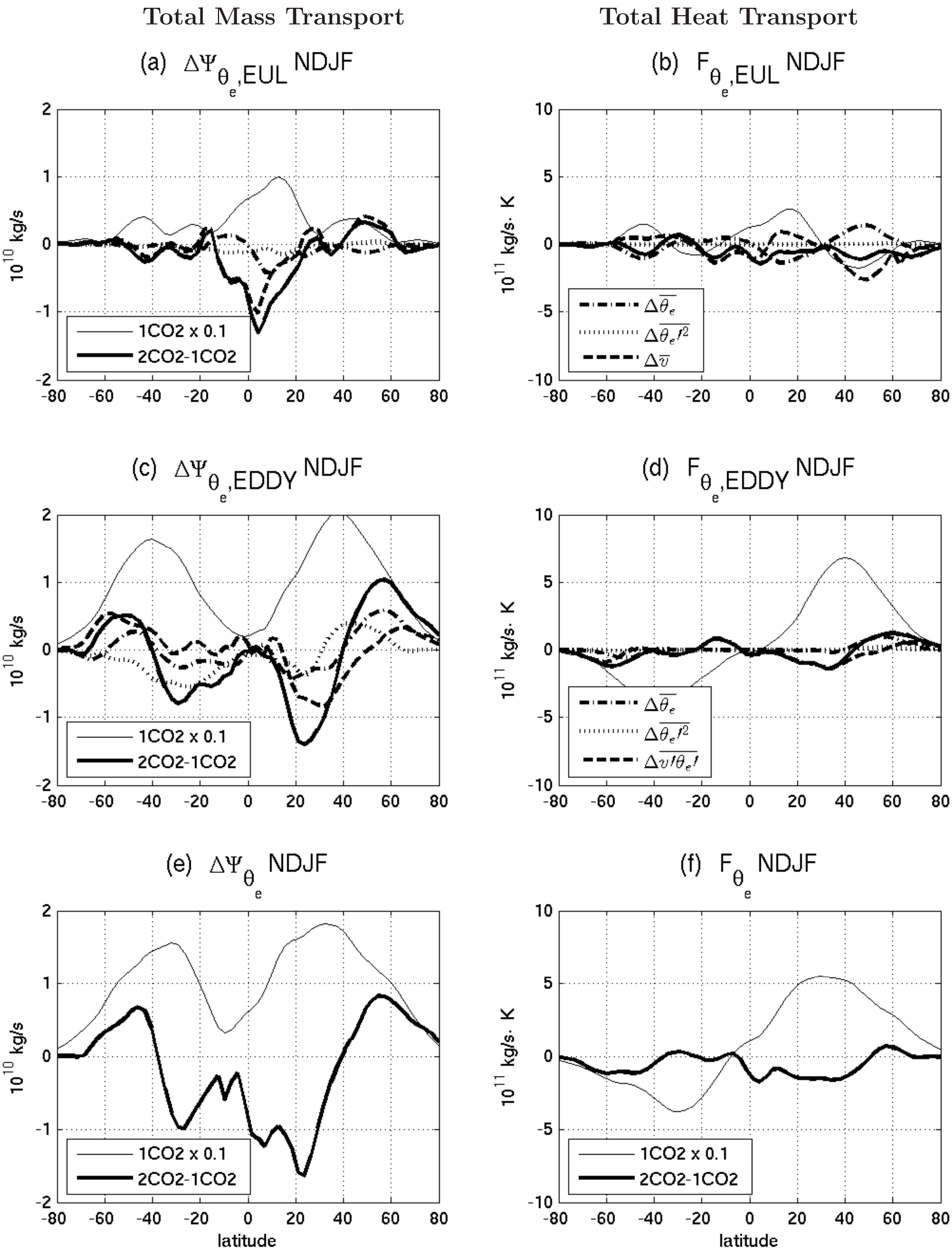

Fig. 5. Same as Figure 4 but for the circulation on moist isentropes.

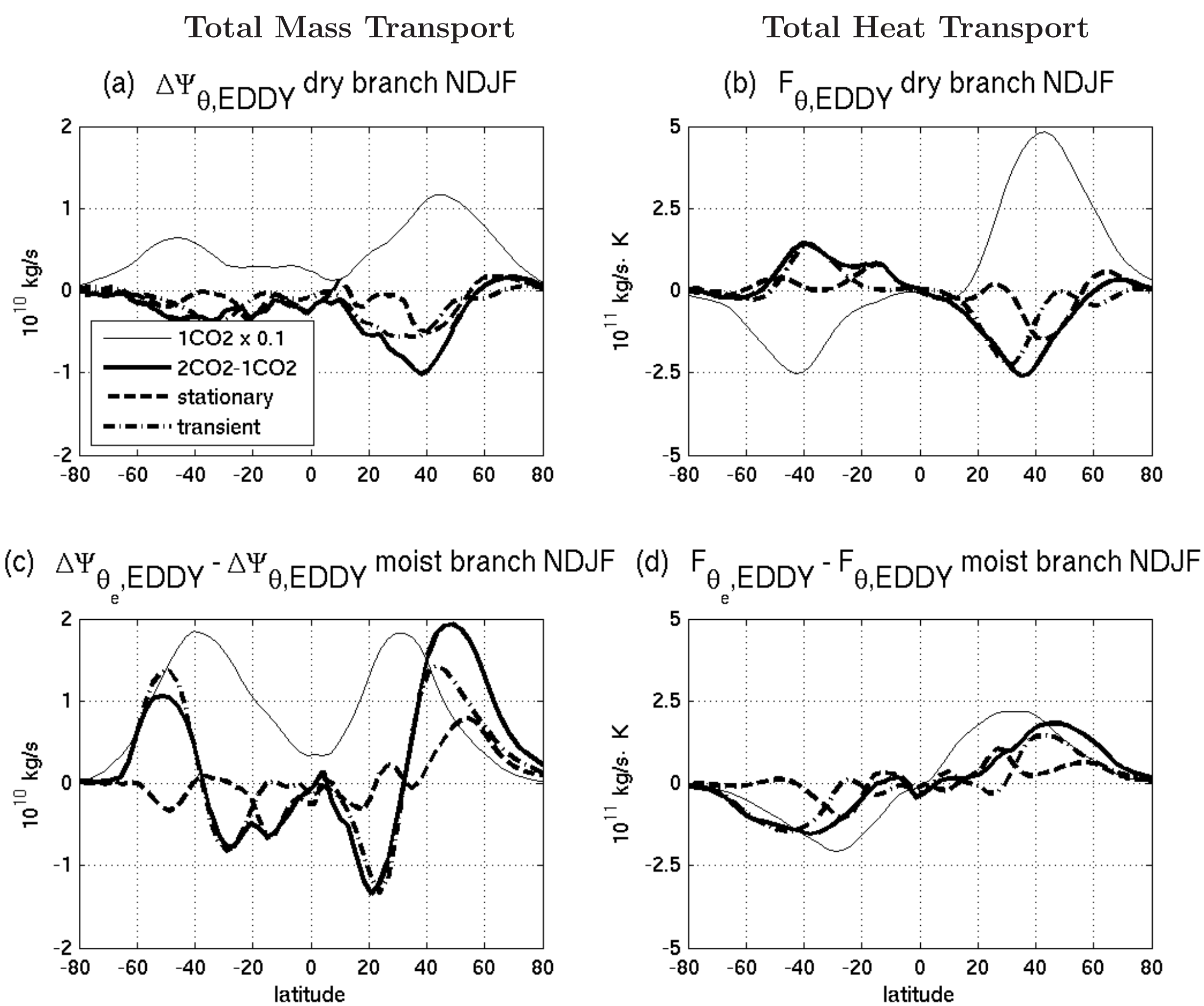

FIG. 6. The doubling CO_2 response (thick solid line) in eddy mass and heat transport in the dry (first row) and moist branch (second row) as well as the decomposition into the stationary (thick dashed line) and transient eddies (thick dash-dot line). The climatologies are plotted in thin solid lines and are divided by a factor of 10.

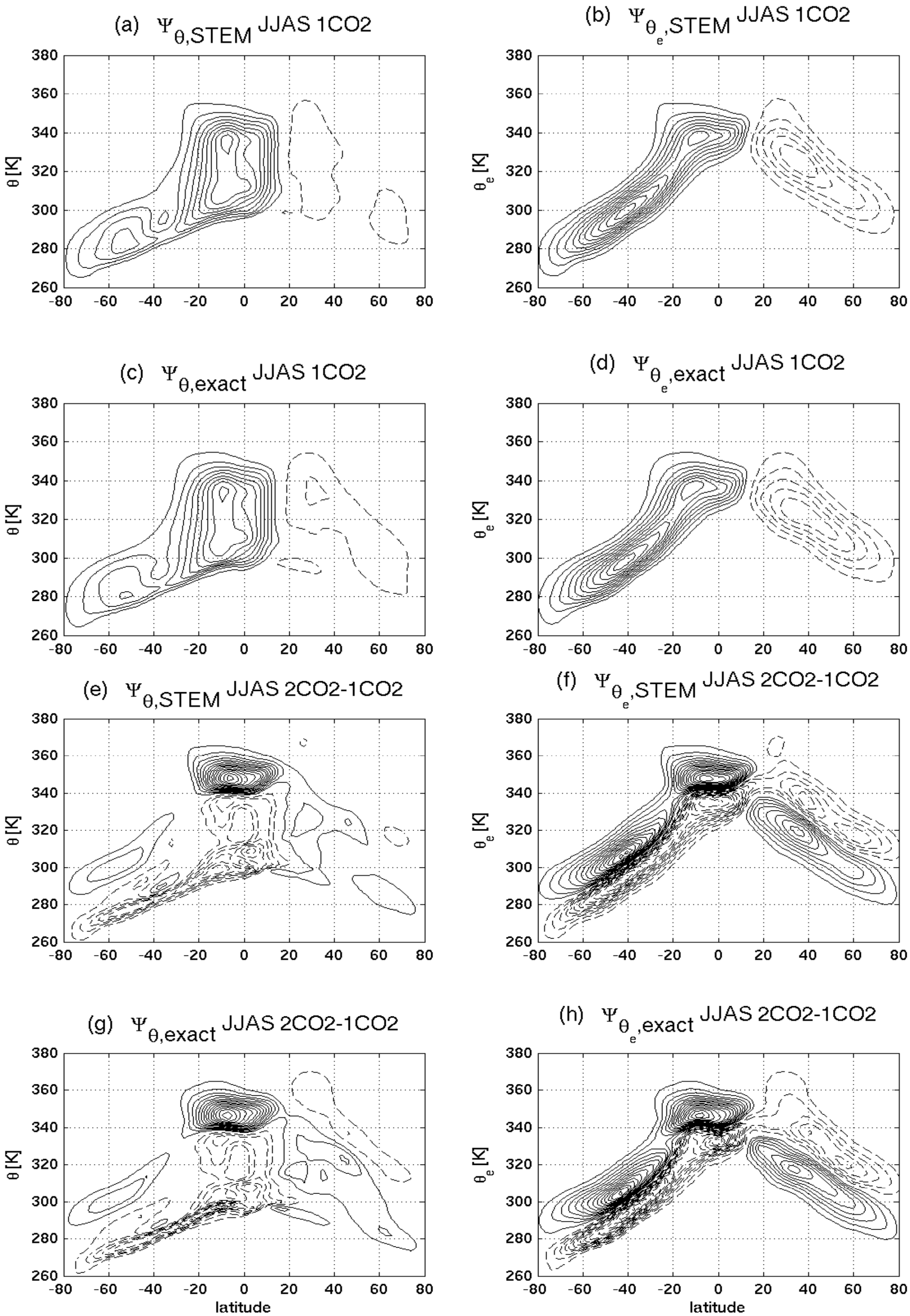

FIG. 7. Same as Figure 1 but for JJAS averages.

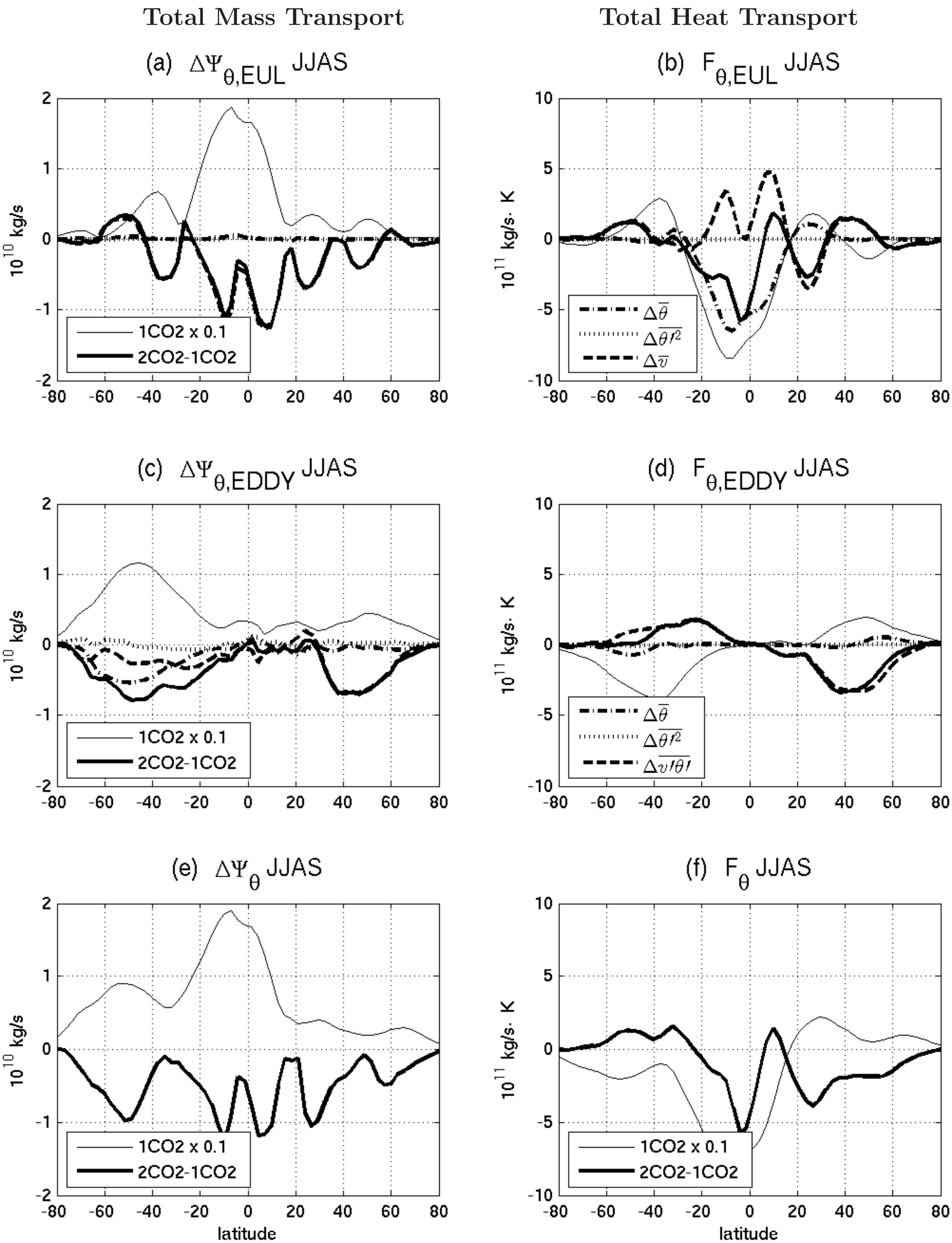

Fig. 8. Same as Figure 4 but for JJAS averages.

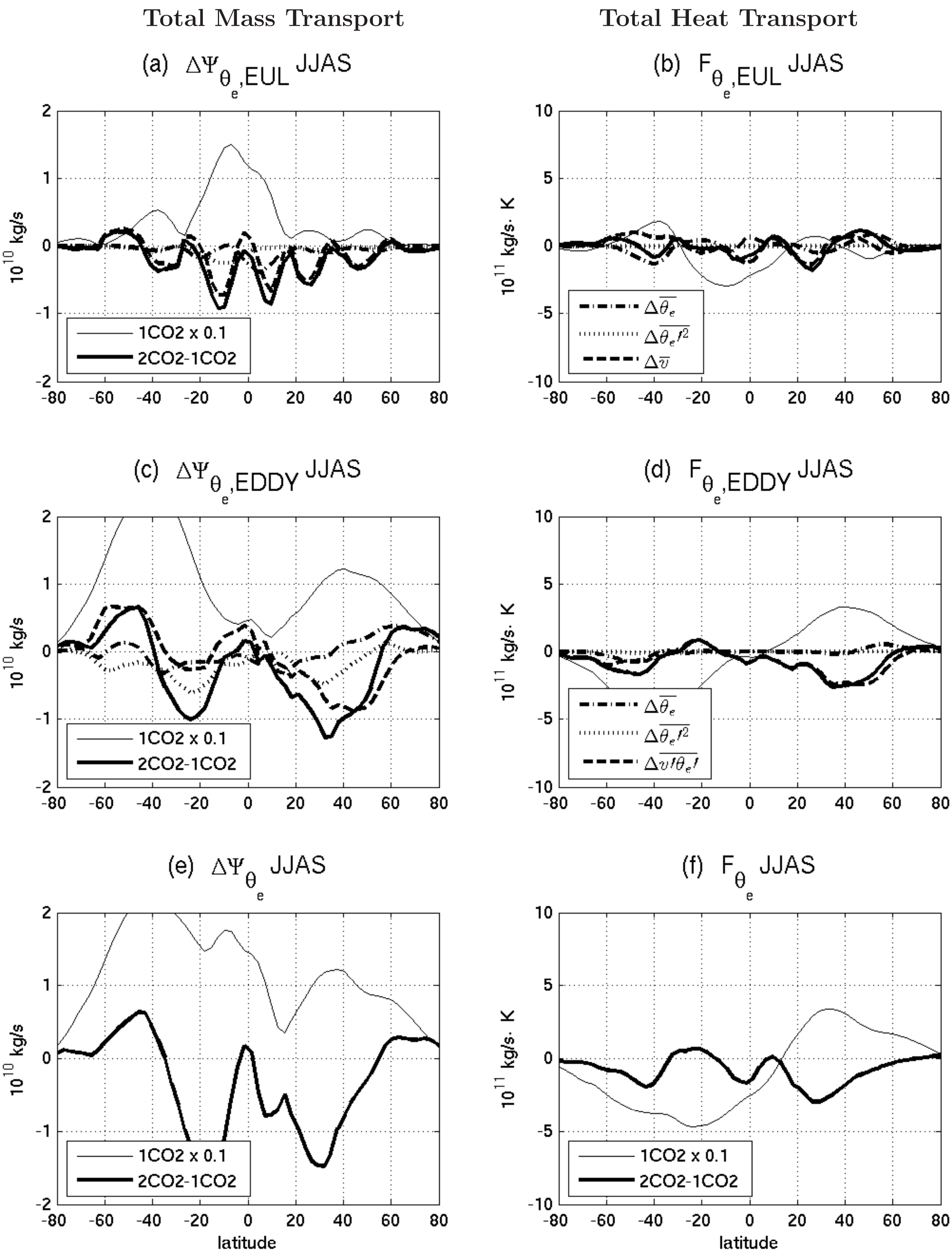

Fig. 9. Same as Figure 5 but for JJAS averages.

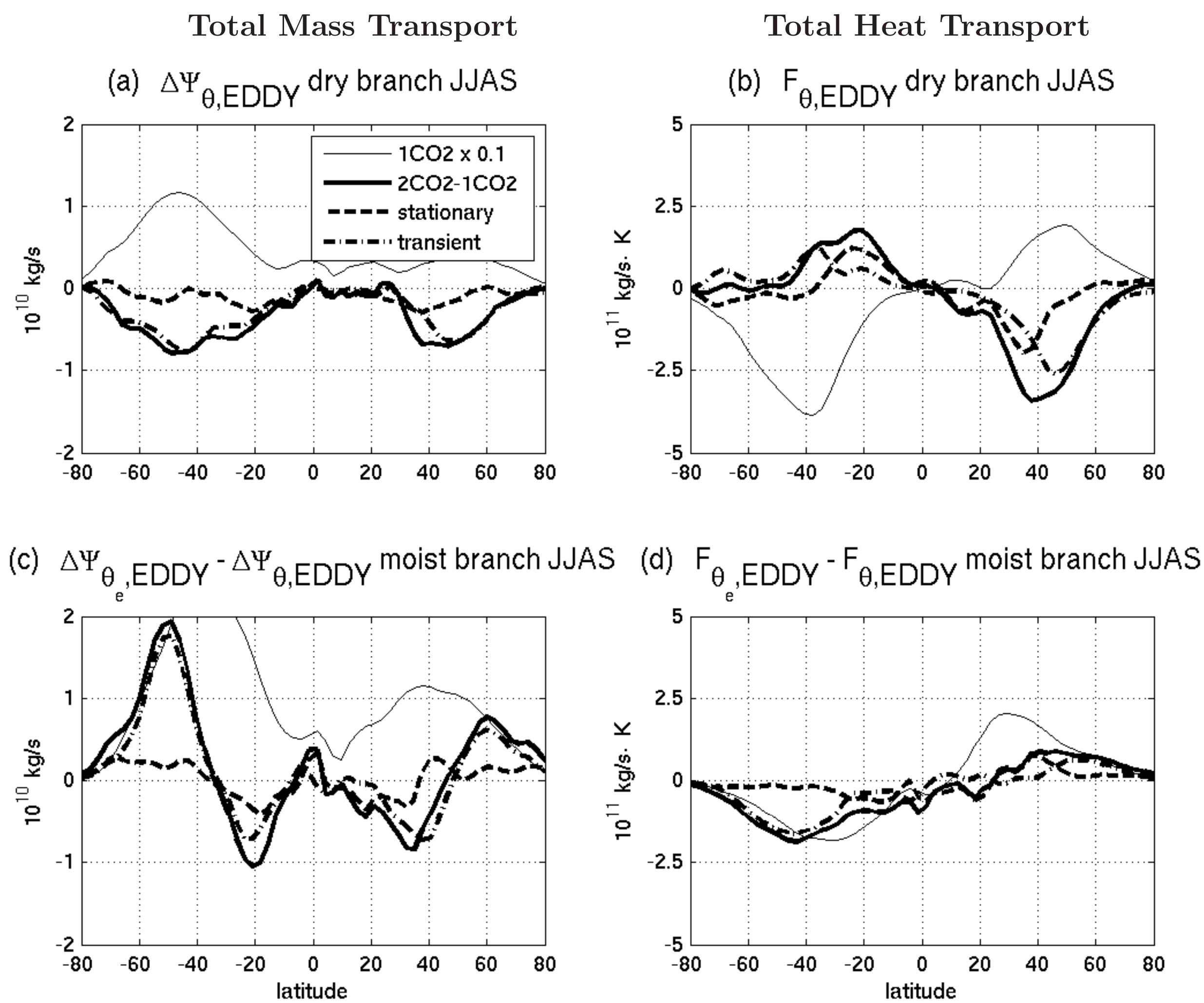

FIG. 10. Same as Figure 6 but for JJAS averages.